

The Growth of Atomically Rough ^4He Crystals

J. Bodensohn, K. Nicolai, and P. Leiderer

Fachbereich Physik, Johannes Gutenberg-Universität, Mainz,
Federal Republic of Germany

Received April 17, 1986

Dedicated to K. Dransfeld on the occasion of his 60th birthday

We have studied the growth of atomically rough bcc and hcp ^4He crystals from the superfluid phase for temperatures $T > 0.9$ K. The growth coefficient displays a temperature dependence which can be represented by $m_4 K \propto e^{\Delta E/k_B T}$. The parameter ΔE is found to be in close agreement with the energy gap of rotons, suggesting that these thermal excitations dominate the growth kinetics. Besides, the absolute value of the growth coefficient depends on crystal orientation, with an anisotropy for the hcp phase of about a factor of 2.5 between the $\{10\bar{1}0\}$ and $\{0001\}$ planes.

I. Introduction

Growing crystals from the melt is very important from the technical point of view and accordingly has been investigated quite thoroughly [1]. A number of mechanisms are involved in the growth process, and in general the topic is rather complex. It is in particular complicated by the fact that in addition to the processes at the interface itself the behavior of the bulk materials - crystal and melt - is of considerable influence, because the latent heat of crystallization has to be carried away from the interface, giving rise to temperature gradients, convection processes etc.

Which growth mechanisms dominate depends primarily on the *structure* of the liquid-solid interface: *i*) For atomically *smooth* interfaces, which on a macroscopic scale appear as facets of the crystal, growth occurs layer by layer from crystal imperfections, like screw dislocations, or from thermally activated nucleation centers. Atomically *rough* interfaces, on the other hand, always provide such an abundance of steps where the atoms from the melt can adjust to the crystal lattice that an activation energy is not necessary there. Consequently crystals with atomically rough surfaces grow rather rapidly; the growth velocity v is proportional to the deviation $\Delta\mu$ of the chemical potential from its equilibrium value μ_0 . For atomically smooth interfaces

such a linear relationship between v and $\Delta\mu$ does not hold [2].

During the past couple of years it has become evident that one of the most suitable substances to investigate crystal growth is helium, in particular the ^4He isotope, because of several coincidences: *a*) Both atomically smooth and rough interfaces can be studied readily, and the transition between these two states at a "roughening temperature" T_R - which for the basal plane of hcp ^4He is at $T \sim 1.25$ K [3, 4] - is easily accessible; *b*) the latent heat of melting is small over a wide temperature range, as is obvious from the nearly vanishing slope of the melting curve; *c*) the thermal conductivity of the superfluid ^4He phase is extremely high. The latter two properties greatly reduce the usual complications caused by heat transport in the bulk materials, so that the crystal growth in this case is dominated by the intrinsic processes at the interface. As a result the relaxation of the solid-liquid interface can become extremely fast, giving rise to intriguing new phenomena such as melting-crystallization waves and a highly anomalous boundary resistance for the transmission of phonons [5-7].

When one is interested in the dynamics of crystal growth, helium offers yet another advantage which is of experimental importance: It is possible to trap negative ions (electron bubbles) at the interface be-

cause this boundary presents an energy barrier large compared to $k_B T$ [8]. Under the influence of an external electric holding field E the ions exert a pressure upon the interface which for large values of E leads to a charge-induced instability of the interface very much like the electrohydrodynamic instability of liquid surfaces [9–11]. In the experiments described here we have made use of the fact that for fields below the instability limit the pressure and hence the chemical potential at the interface can be varied rapidly and in a very subtle and well-defined way by changing the holding field. The resulting response of the crystal-superfluid interface then yields the desired information about the growth velocity, metastable states, anisotropy effects etc., which will be discussed below. Preliminary results have already been presented earlier [10, 11].

II. Experimental

A crystal of solid ^4He at $T > T_R$ develops a convex meniscus, similar to a liquid which does not wet the walls of the sample cell.* The central part of the crystal surface is essentially horizontal and flat and it is this portion of the interface that was studied with our technique by means of the charges.

A sketch of the sample cell is shown in Fig. 1. Its diameter is 40 mm, and the spacing between the bottom and top glass plates is 20 mm. The plates serve two purposes:

i) For one, they form a horizontal capacitor which provides the electric field to manipulate the probe charges. They are therefore covered with conductive coatings, a transparent In_2O_3 layer for the bottom and a gold mirror for the top plate, to which a potential difference can be applied.

ii) Simultaneously the plates constitute an interferometer which is used to detect minute changes in the shape of the crystal surface during the growth or melting process. Optical access to the cell is from below through windows in the bottom of the cryostat.

The electron bubbles are produced in the upper part of the cell in the liquid phase by a field emission tip and pulled downwards to the crystal-liquid interface by means of the externally applied electric field E [11]. At the interface they are trapped with a typical density n of about 10^8 cm^{-2} . The average interparticle spacing is then $\sim 10^4 \text{ \AA}$, so that a noticeable change of the interfacial properties due to the ions is not expected.

* For some wall materials, like graphite, wetting can occur [12, 13]

When the ions exert an electrostatic pressure on the interface, a thin layer of the crystal melts. This at the first sight somewhat surprising observation is explained in the following way: Since the electronic pressure only acts on the solid phase (which presents the potential barrier for the charges), the chemical potential of the solid is increased. The chemical potential of the liquid, on the other hand, is not altered by the charges. Consequently the energy of the system is lowered when a certain portion of the solid is transformed into the liquid state. Equilibrium is attained at a depth ζ_0 , where the electrostatic pressure P_{el} is balanced by the hydrostatic pressure, i.e. when

$$\Delta \rho g \zeta_0 = P_{el}. \quad (1)$$

Here $\Delta \rho$ is the difference of the density between the liquid and solid phase. Effects of the interfacial tension have been neglected in (1), because we are studying deformations of the interface on a scale large compared to the capillary length (which is about 1 mm for the hcp-superfluid ^4He interface) [11]. Since the heat produced with our technique is exceedingly small, temperature differences can be neglected as well.

The new equilibrium position of the crystal surface is reached with a characteristic relaxation time τ , which is a measure of the speed of *melting*. Similarly, information about the *growth* is obtained from the relaxation back to the original crystal position as the electric field is reduced to the starting conditions.

In order to measure the motion of the interface we have used the optical set-up also shown in Fig. 1. The sample cell is illuminated by the expanded beam of a He-Ne laser, attenuated to 10^{-5} W to avoid heating of the walls. The interference pattern resulting from the superposition of light reflected from the top and the bottom plate is magnified by lens L_3 and can be viewed on the screen S (see Fig. 2). In the regions where the crystal melts or grows the interference fringes move, a shift by one fringe corresponding to a change in crystal height of

$$\Delta \zeta = \lambda/2 \Delta n. \quad (2)$$

Here λ is the laser wavelength and Δn is the difference between the refractive indices of the liquid and the solid phase. With $\lambda = 632.8 \text{ nm}$ and $\Delta n = 0.0034$ we obtain for $\Delta \zeta$ a value of $93 \mu\text{m}$. The resolution that can be attained is considerably higher, however. We have used two modifications of the interference technique to register relatively large and small variations, respectively. The principles are sketched in Figs. 3 and 5.

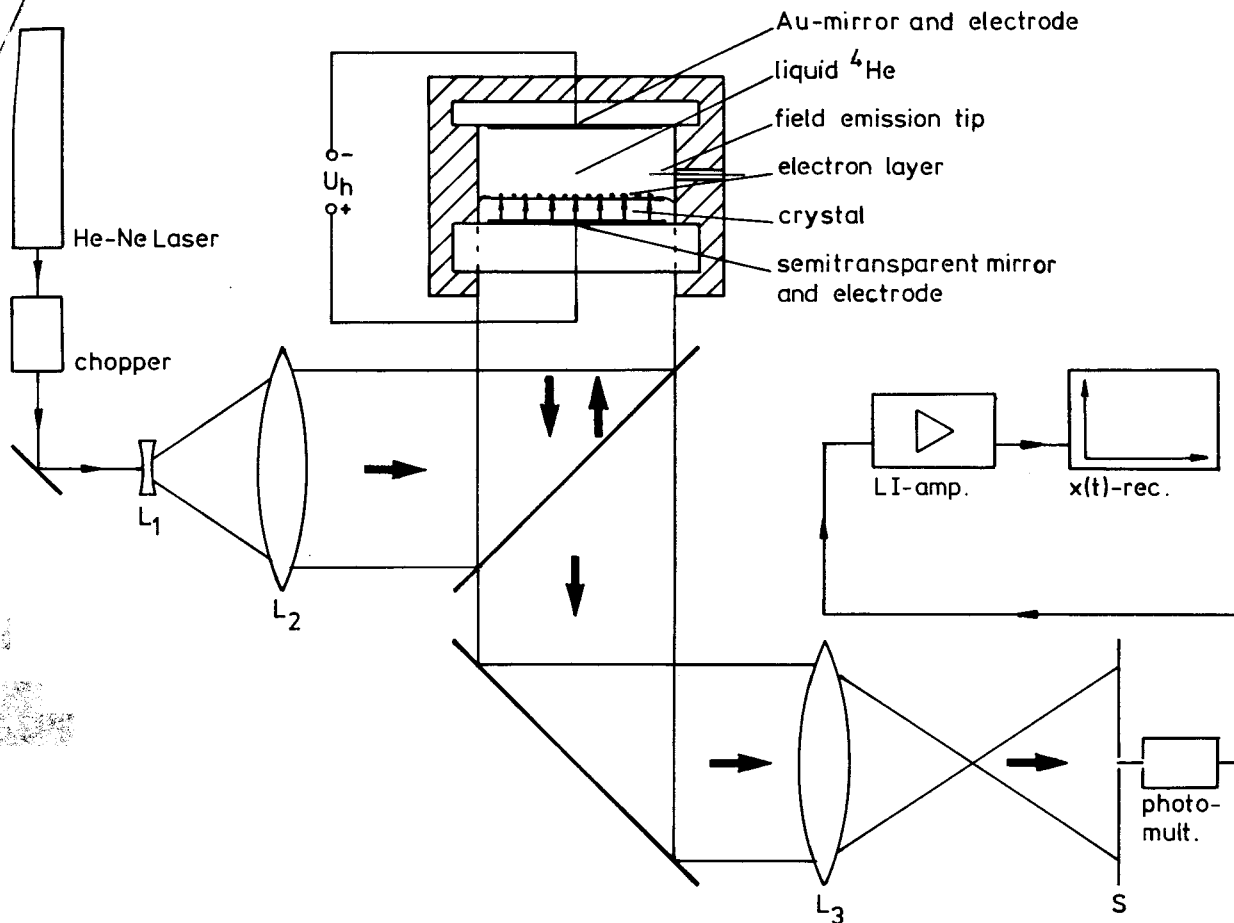


Fig. 1. Optical set-up and sample cell. The He-Ne Laser beam is expanded by the lenses L_1 and L_2 and is reflected into the sample cell by a semitransparent mirror. Lens L_3 produces an image of the cell on the screen S . Changes in the interference pattern of the cell are detected with high spatial resolution by a combination of a photomultiplier and a thin glass fibre, which can be moved in the image plane



Fig. 2. Interference pattern of a charged hcp-superfluid ^4He interface [8]. The field of vision has a diameter of 2 cm. In this example the ions are concentrated in the middle of the cell to enhance the visibility of the deformation (The parallel fringe pattern outside the center results from a slight inclination of the two interferometer plates). For actual measurements, the ion distribution at the interface was chosen much more homogeneous by properly adjusting the electrostatic potentials applied to the walls of the cell

a) Large Changes in Height

We measure the response of the crystal surface to a square wave variation of the electric field superimposed on the applied dc field. When the amplitude of the field variation is large and the crystal layer which melts or solidifies is of the order of several hundred μm , the interference pattern shifts by more than 1 fringe. The lower trace in Fig. 3 shows the signal from a small photodetector (diameter $\ll 1/2$ fringe width) positioned in the image plane. The maxima and minima correspond to the passage of bright and dark portions of the interference pattern. Consecutive maxima therefore are equivalent to a change in height of $93 \mu\text{m}$, as expressed by Eq. (2). The change of the position of the crystal surface as derived from the intensity variation is plotted in Fig. 4.

b) Small Amplitudes

For small amplitudes of the electric field and correspondingly small ($\zeta_0 \ll 100 \mu\text{m}$) variations of the

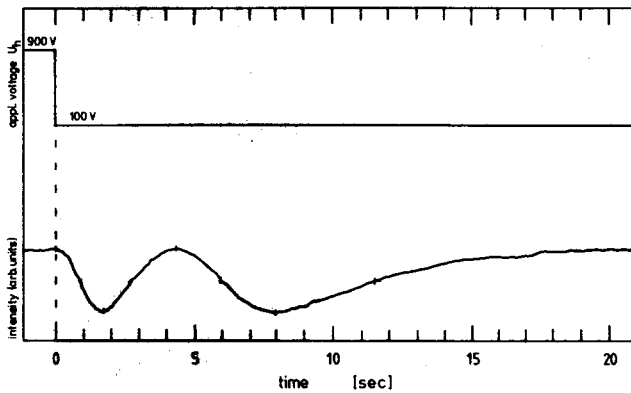


Fig. 3. Relaxation of an hcp-superfluid ^4He interface ($T = 1.25\text{ K}$). At time $t = 0$ the electric field is reduced from 900 to 100 V, and the crystal starts to grow, as seen from the variation of the light intensity detected by the photomultiplier. The passage of about 2 interference fringes corresponds to a growth of the crystal of $190\ \mu\text{m}$

crystal height the photodetector signal does no longer pass through several maxima and minima, but covers only a fraction of the nearly sinusoidal sensitivity curve of the interference device. By properly adjusting the position of the detector (roughly in the middle of the transition between a dark and bright fringe) it is possible to achieve a nearly linear response of the photodetector to changes in the crystal height (Fig. 5).

Using a lock-in technique with a chopped laser beam we have reached a resolution for variations of the crystal height of better than $0.5\ \mu\text{m}$. This allows

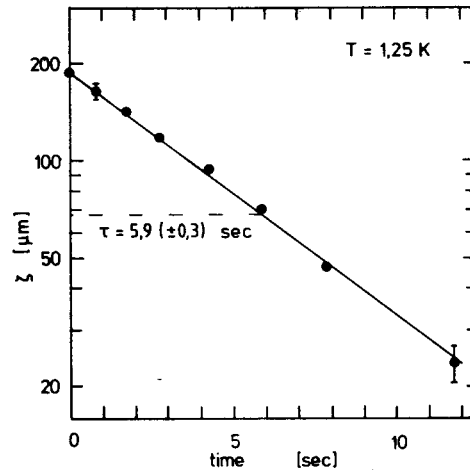


Fig. 4. Position of the crystal-superfluid interface vs. time as derived from the relaxation process in Fig. 3

one to measure the behavior of crystal growth even for extremely small deviations Δp from the equilibrium pressure p_m at the melting curve (the ratio $\Delta p/p_m$ can be as small as 10^{-10}). The lateral resolution of the interference pattern, limited by the imaging optics, is about $0.1\ \text{mm}$.

III. Results and Discussion

For all our measurements we have used commercial ^4He with an estimated ^3He impurity concentration

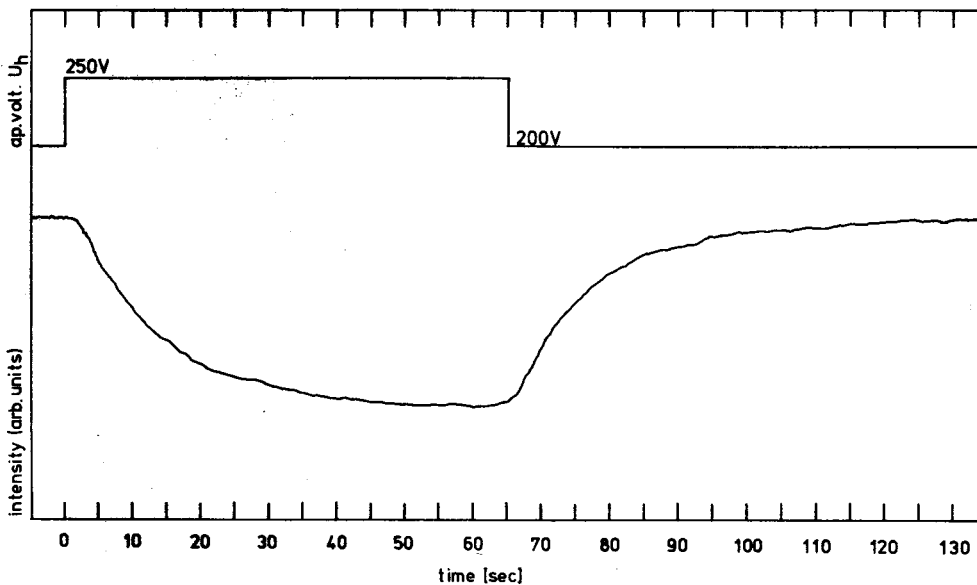


Fig. 5. Same as in Fig. 3, however with a smaller change in the electric field and a correspondingly reduced variation of the crystal height ($T = 1.35\text{ K}$). The change in light intensity here is proportional to ζ . In addition to the growth also the melting process, occurring after an increase of the electric field, is shown

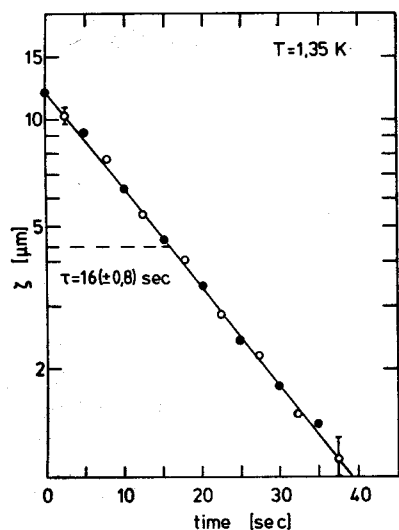


Fig. 6. Position of the crystal-superfluid interface vs. time as derived from the relaxation process in Fig. 5. Open symbols refer to growth, and closed symbols to melting. The relaxation times for both processes are the same, as expected when the deviations from equilibrium are small

of about 10^{-7} . Before we discuss the results for crystal growth obtained with charged crystal surfaces, we first describe some observations for uncharged crystals.

Uncharged Solid-Liquid Interface

It has been observed already in the early experiments on helium crystal growth that while growing the crystals differ from their equilibrium shape. An example is given in Fig. 7 which shows a crystal at $T=1.35$ K oriented with its c axis nearly perpendicular to the viewing plane. In equilibrium (Fig. 7a) one notes hardly any anisotropy in the crystal contour, as expected for temperatures above T_R . As soon as helium is added to the sample cell and the crystal grows, however, a distinctly anisotropic shape develops, which displays the hexagonal symmetry of hcp He (Fig. 7b). Figures 7c and d show a similar behavior for another crystal orientation.

At the first glance the boundaries of the growing

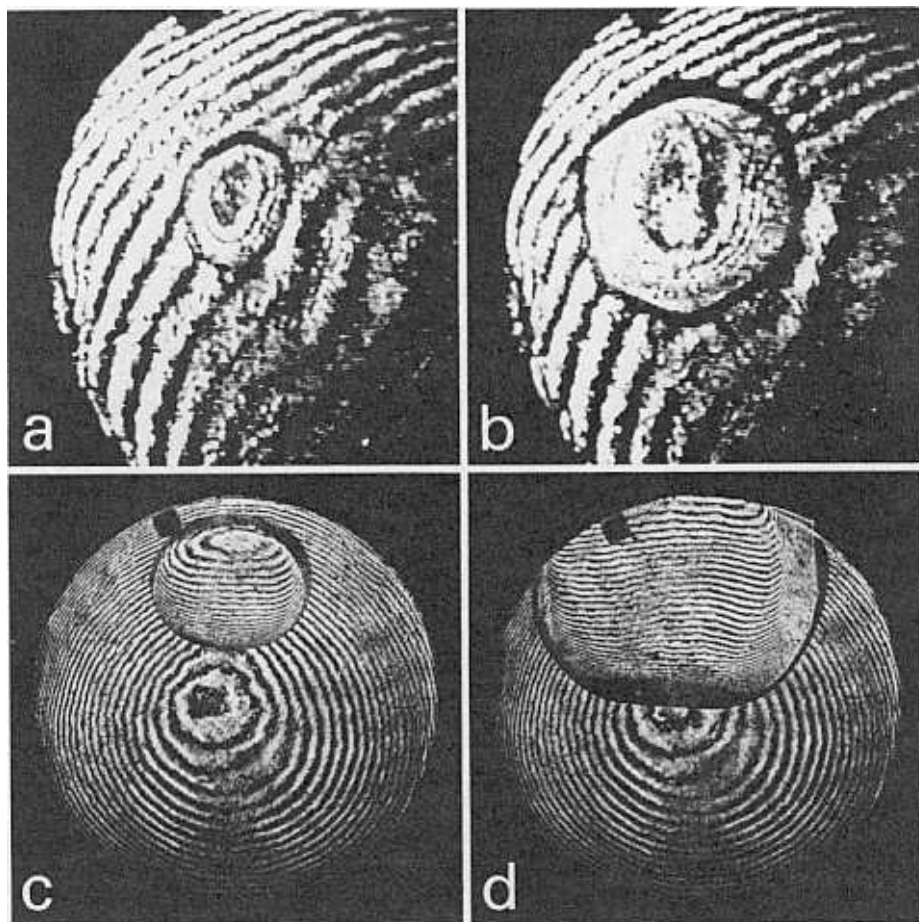


Fig. 7a-d. hcp ^4He crystals at 1.35 K in equilibrium (a, c) and during growth (b, d)

crystals appear as plane facets, as they develop for atomically smooth surfaces below the roughening temperature. Yet a closer inspection reveals that these apparent facets are still curved. They are caused by an asymmetry in the growth coefficient, and disappear when the growth is stopped and the crystal is allowed to relax towards its equilibrium shape.

Absolute values for the growth coefficient are difficult to determine from studies as shown in Fig. 7, because the overpressure and hence the chemical potential difference, $\Delta\mu$, with respect to the melting curve are not known with adequate accuracy when He is added through the sample cell capillary. What is possible, however, is to obtain an estimate for the *anisotropy* of the growth coefficient for various crystal directions. For instance, for a crystal with a horizontal basal plane like in Fig. 7a, b the ratio of the growth velocities in the $\langle 11\bar{2}0 \rangle$ and $\langle 10\bar{1}0 \rangle$ directions can be derived from the change in the crystal contour, whereas the simultaneous growth in the $\langle 0001 \rangle$ direction perpendicular to the image plane follows from the shift of the interference fringes. From an analysis of our data we get for the growth velocities at 1.35 K

$$v_{\langle 11\bar{2}0 \rangle} : v_{\langle 10\bar{1}0 \rangle} : v_{\langle 0001 \rangle} = 2.8 : 2.5 : 1. \quad (3)$$

This result has to be compared now with quantitative measurements obtained with ions trapped at the crystal surface.

The Charged hcp-Superfluid Interface

We first discuss results for rough hcp surfaces. When a steplike perturbation is applied to such an interface by switching the electric holding field, the position of the interface approaches the new equilibrium exponentially. This was found to hold over the whole investigated range of amplitudes $0.5 \mu\text{m} \leq \zeta_0 \leq 0.5 \text{mm}$, as shown in Figs. 4 and 6:

$$\zeta = \zeta_0 e^{-t/\tau}. \quad (4)$$

Equation (4) can also be written as

$$\dot{\zeta} = -\frac{1}{\tau} \zeta. \quad (5)$$

Since $\dot{\zeta}$ is the growth velocity v , and $\zeta = \Delta\mu\rho_c/g\Delta\rho$, we have

$$v = -\left(\frac{\rho_c}{g\Delta\rho\tau}\right) \Delta\mu \quad (6)$$

where ρ_c is the density of the crystal.

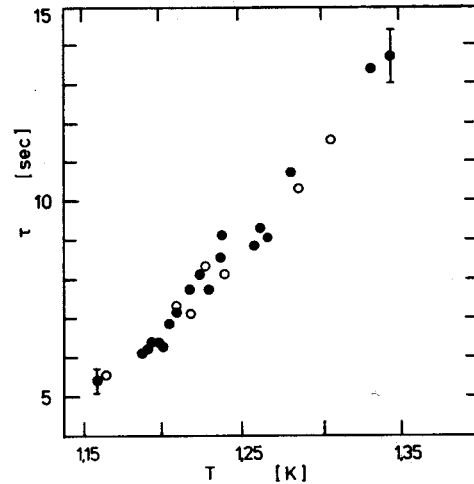


Fig. 8. Relaxation time τ of an hcp crystal vs. temperature. Open symbols: temperature increasing, closed symbols: temperature decreasing

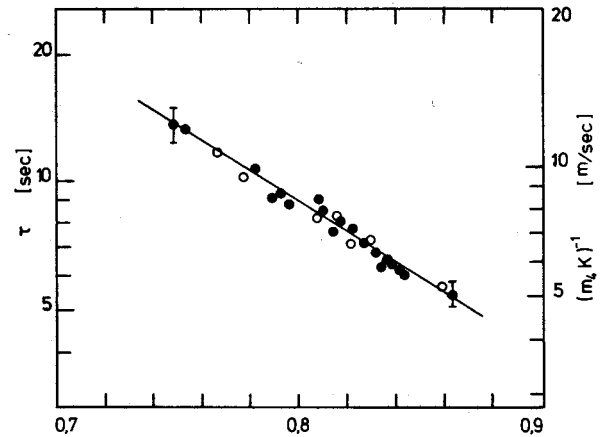


Fig. 9. Same data as in Fig. 8, but on different scales. A $\log \tau$ vs. T^{-1} plot is motivated by the comparison with data covering a wider temperature range (see Fig. 11). The solid line represents a temperature dependence $\tau \propto \exp(-\Delta E/k_B T)$ with $\Delta E/k_B = 8.1 \text{K}$. The kinetic growth coefficient ($m_4 K$) is related to τ by Eq. (7)

Thus the relaxation time τ measured in our experiment is related to the kinetic growth coefficient ($m_4 K$), defined by $v = -(m_4 K) \Delta\mu$, by

$$\tau^{-1} = (m_4 K) g \Delta\rho / \rho_c. \quad (7)$$

According to (6) the growth velocity is proportional to $\Delta\mu$ as expected for an atomically rough surface. But what are the processes which limit the crystal growth in the case of He? A clue can be obtained by studying the temperature dependence of the relaxation time:

In Figs. 8 and 9 this dependence is plotted on two different scales for a crystal with random orientation (neither the c - nor the a -axis being vertical).

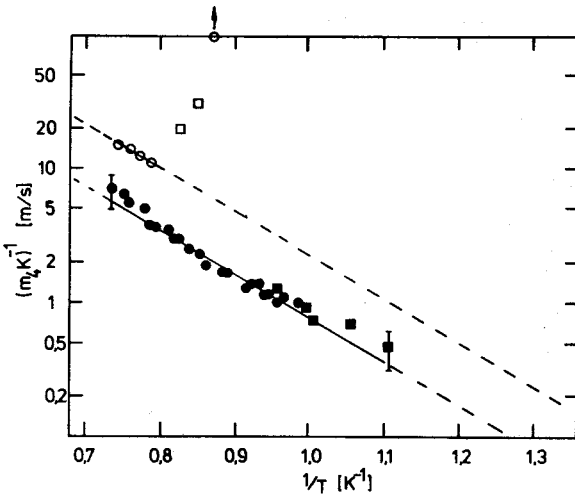


Fig. 10. Inverse growth coefficients of several hcp crystals with [0001] (open symbols) and [1010] (closed symbols) orientation. Relaxation times for intermediate crystal orientation were found to lie between the two straight lines. The slopes in this case corresponds to $\Delta E/k_B = 7.3$ K. Data for the (0001) plane below 1.25K refer to initial slopes of the relaxation curves and are only intended to give an impression of the time scale of crystal growth, because the relaxation process in this range is no longer exponential

No dependence on the sample history was observed, as is indicated by the nearly identical data taken during slowly cooling down and warming up. Obviously the relaxation of the crystal surface towards the equilibrium position develops faster as the temperature is lowered. This rules out thermally activated processes such as nucleation to dominate crystallization in this case, because these would lead to just the opposite temperature dependence. The straight line in Fig. 9 suggests a relation

$$\tau \propto (m_4 K)^{-1} \propto e^{-\Delta E/k_B T}. \quad (8)$$

(The slight temperature dependences of $\Delta\rho$ and ρ_c which according to Eq. (7) enter the relation between τ and $(m_4 K)^{-1}$, can be neglected here.) Data for other crystal surfaces show the same behavior, with $\Delta E/k_B = 7.6 \pm 0.5$ K, irrespective of the orientation. An exception are {0001}-surfaces below about 1.25 K, as seen in Fig. 10. This point, which apparently is related to the roughening transition of the basal plane, is to be discussed later.

The observed dependence of the growth coefficient on temperature is in very good accord with data at lower temperatures, obtained by other groups from melting-crystallization waves [5] and sound transmission through the interface [6, 14]. A comparison of these results for the different techniques is given in Fig. 11, showing the very wide

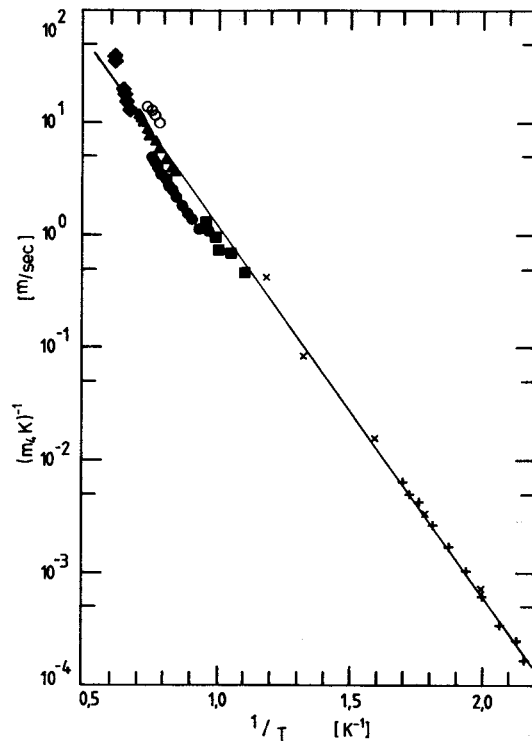


Fig. 11. Inverse growth coefficient of solid ⁴He. + Keshishev et al., Ref. 5; x Castaing et al., Ref. 6; this work: o hcp, [0001]; ●, ■ hcp, [1010]; ▲, hcp, arbitrary orientation ◆, bcc (cf. Fig. 12). The slope of the full line corresponds to $\Delta E/k_B = 7.6$ K, which is close to the value 7.8 K quoted by Keshishev et al. for the low temperature data. The difference to the real roton gap (7.2 K) has been ascribed to a temperature dependence of the preexponential factor [5]. The phonon contribution to the growth resistance, which becomes important at low temperatures, has been subtracted here

range of the growth coefficient accessible with He crystals.

It has been suggested already in the early work of Keshishev et al. [5] that the growth in ⁴He at low temperatures is dominated by phonons and rotons. In the region that we have investigated, $T > 0.9$ K, the phonon contribution is negligible compared to the rotons. The observed dependence (8) therefore agrees very well with this picture, because a relation similar to (8) with the same ΔE governs the number of rotons in liquid ⁴He.

Theories which relate the growth coefficient to the thermal excitations in the bulk phases have been presented by Andreev and Knizhnik, and by Bowley and Edwards [15, 16]. The basic idea there is that the growth velocity is limited by the reflection of phonons and rotons from the solid-liquid boundary because the quasiparticles are changed in their distribution when reflected from a moving interface. This gives rise to a production of entropy and there-

fore leads to a resistance to growth. In their original form these theories yield the experimentally observed temperature dependence of the kinetic growth coefficient – a contribution from rotons varying as $e^{-7.8/T}$, from phonons as T^{-4} [5] – only for relatively low temperatures where the excitations propagate ballistically in the bulk phases. In the higher temperature ($T \gtrsim 0.6$ K) “hydrodynamic” regime, however, where all our measurements have been made, the growth coefficients predicted by the above mentioned theories strongly deviate from the experimental data.

In order to resolve this discrepancy Bowley and Edwards consider mechanisms which might bring the roton gas to rest in the frame of the lattice rather than the interface, restoring for the growth coefficient in the hydrodynamic regime the same behavior as in the ballistic range [16]. This aspect has been discussed in more detail by Castaing [14], who proposed that one should take into account the order induced in the liquid in the vicinity of the solid surface, an effect suggested by molecular dynamics calculations [17]. Then the resulting scattering potential for rotons becomes long-ranged and can no longer be reduced to a static potential in the frame of reference of the moving interface. As a consequence the treatment by Bowley and Edwards should apply even in the hydrodynamic regime.*

A result which might support this picture is the dependence of the growth coefficient on the crystal orientation. As seen from Figs. 10 and 11, the temperature dependence of $m_4 K$ for different crystals is the same, but the absolute value can vary. Originally this was ascribed to variations in the crystal quality. Studies on oriented crystals have shown, however, that the apparent scatter is due to the crystal anisotropy. The value of $(m_4 K)^{-1}$ measured for the relaxation of the basal plane is more than twice the value for the $\{10\bar{1}0\}$ plane at the same temperature. This agrees well with the growth anisotropy found for the uncharged crystals. If, as suggested by Castaing, the roton reflection at the solid-liquid interface is dominated by the order which extends from the solid into the liquid phase, such an anisotropy can qualitatively be understood: Since the periodicity of the induced order is expected to depend on crystal orientation (similar to the reciprocal lattice vector of the solid perpendicular to the interface), the “matching” of the roton wave vector to that periodicity and hence the roton scattering at the interface should depend on the orientation as well.

As already mentioned the growth coefficient of the basal plane appears to be qualitatively different

* An alternative explanation for the surface mobility, which is based on the collision of rotons with surface kinks, has been given by Wolf et al. [3]

from the other orientations in that the relaxation time starts to increase below about 1.25 K, and rapidly exceeds the limit which can be reached with our set-up (~ 1 min). Simultaneously the relaxation of ζ begins to deviate from an exponential (so that a well defined value of τ does no longer exist), leading to hysteresis effects and metastable states.

It has been shown already by Balibar et al. that this change in behavior is related to the roughening transition of the basal plane [3]. Below T_R the number of thermally activated steps drops quickly and a plane, macroscopic facet develops.

The crystal growth for the facet is limited by processes like the 2-dimensional nucleating of layers; compared to these the contribution of roton reflection to the growth resistance becomes negligible. The steep increase of τ in this regime reflects the slowing down of the nucleation process for decreasing T . Similar behavior is expected for other crystal surfaces at the corresponding roughening transitions, e.g. at 0.85 K for the $\{10\bar{1}0\}$ and at 0.36 K for the $\{10\bar{1}1\}$ surfaces [18].

We note that for crystal surfaces whose orientation is close (say, within a few degrees) to the plane of a facet the relaxation may develop in a somewhat more complex way than described earlier. As soon as a facet is present on some part of the crystal surface – which for such orientations is very likely – the motion of the adjacent rough areas is coupled, due to the surface tension, to the very slow relaxation of the facet. The response of the crystal surface to the switching of the external electric field will then no longer be spatially homogeneous, as above T_R , but will depend on the distance to the facet boundary. The detailed behavior in this regime below the roughening transition will be the subject of a separate paper.

The Charged bcc-Superfluid Interface

Data for two different bcc crystals (orientation not determined) are plotted in Fig. 12, where for comparison also results for a hcp crystal are shown. In the temperature range where the bcc phase is stable the roton energy Δ , can no longer be considered as being constant. Hence the solid curve in Fig. 12, which represents a dependence $\propto e^{-\Delta/k_B T}$ (cf. Eq. (8)), deviates from a straight line. (The values of Δ , used here have been extrapolated from data of Dietrich et al. [19] to the melting curve.) As for the hcp phase, the temperature dependence given by Eq. (8) yields a good fit to the data. Moreover, also the absolute values of the growth coefficient for the bcc phase agree quite well with the extrapolated hcp results. The crystal growth of the cubic phase therefore appears to be dominated by the same process as

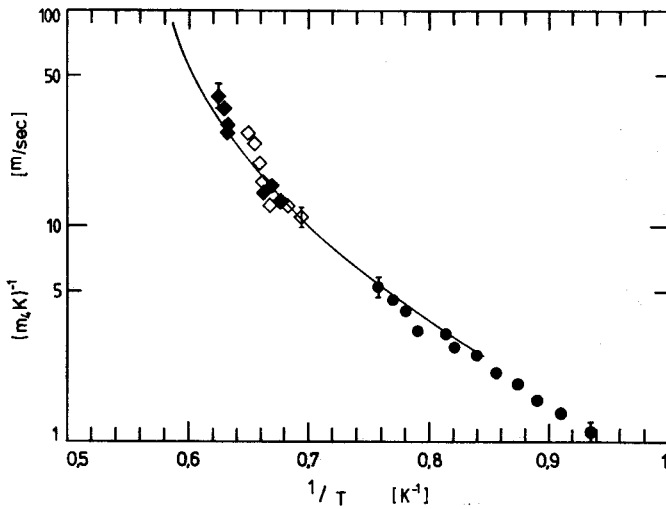


Fig. 12. Inverse growth coefficient of two bcc ^4He crystals (\diamond , \blacklozenge). For comparison, data for the $(10\bar{1}0)$ surface of hcp ^4He are also shown (\bullet). The solid curve indicates a temperature dependence proportional to $e^{-\Delta_r/k_B T}$, where Δ_r is the roton energy gap

for the hexagonal phase, which indicates that the crystal structure is of minor importance. This can be considered as an additional support for the idea that the growth resistance is essentially due to the reflection of rotors not only in the ballistic, but also in the hydrodynamic, high temperature regime.

Valuable additional information about the mechanisms involved in the growth process and in particular about the role of the liquid phase should become available from studies at even higher temperatures ($T > 1.8\text{ K}$). There the crystal again has hcp structure, but the liquid is normal instead of superfluid. Preliminary studies have shown that growing crystals with sufficient surface quality is tedious at these high temperatures because of the tendency

towards dendritic growth. An alternative way to approach this interesting region may be to grow the hcp crystal from the superfluid phase, and circumvent the bcc phase by first applying sufficient pressure ($p \gtrsim 31\text{ bar}$) and then increasing the temperature until the melting curve is reached. In this range, then, the crystal growth should be governed by the same processes as in other normal van der Waals systems.

Development of Surface Deformations During Cooling

Finally, we report on an observation which we have made for crystal surfaces during rapid cooling. No matter how flat the surface is in thermal equilibrium, it deforms spontaneously when the sample is cooled, such that a quasi-periodic pattern develops as illustrated in Fig. 13. The characteristic distance of the corrugations, 6 mm , is close to $2\pi a$, where $a = (\bar{\alpha}/g\Delta\rho)^{1/2}$ is the capillary length, and $\bar{\alpha}$ is the interfacial tension [11]. The preferential direction of the corrugations is parallel to the pseudo-facets observed for the same crystal during the initial growth process and is hence apparently determined by the crystal anisotropy.

This phenomenon is reminiscent of the electrohydrodynamic instability observed at high electric fields for liquid-gas as well as solid-liquid interfaces as a result of ripplon softening [8-11]. The structure here cannot be caused by the same mechanism, however, because it develops irrespective of whether the interface is charged or not and independently of the applied electric field. Rather the origin must be related to the temperature gradient present in the sample during cooling. This is corroborated by the observation that as soon as the crystal is in thermal equilibrium again the corrugations diminish and the

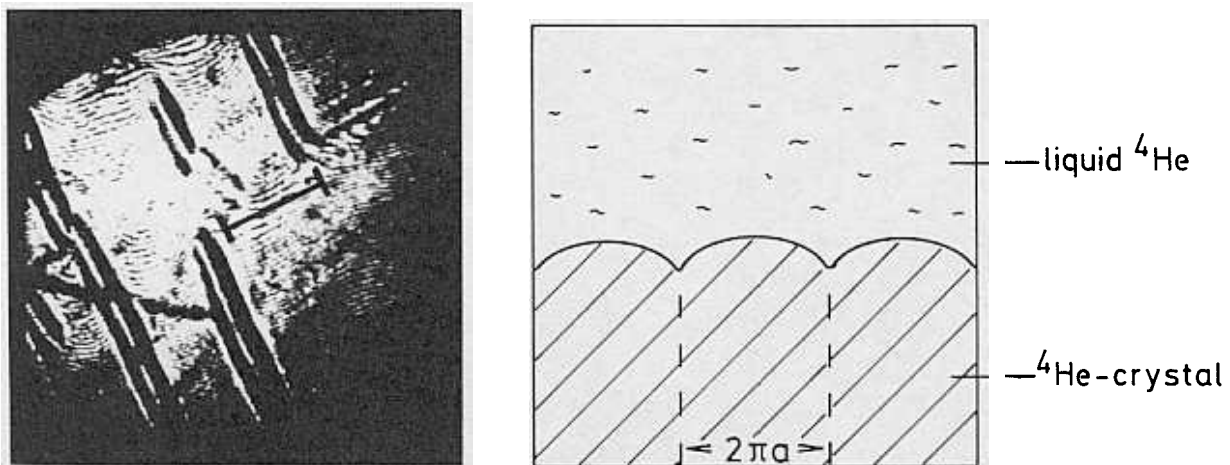


Fig. 13. a Interference pattern of an uncharged hcp-superfluid ^4He interface, for a sample cooled at a rate of 20 mK/min . The length of the scale bar is equal to $2\pi a = 6.3\text{ mm}$. b Schematic cross section of the interfacial profile shown in a

original smooth surface is retained. A qualitative argument which might explain the formation of the corrugations is as follows: Since our sample is cooled from the top, the flow of heat is directed upwards when the temperature is lowered. This will give rise to a temperature gradient in the solid and a discontinuity at the interface due to the Kapitza boundary resistance. Temperature gradients in the liquid are very small because of the extraordinary thermal conductivity of the superfluid phase in this temperature range. Assume now that fluctuations have led to a small local depression of the interface. In the presence of a heat flow the temperature at the solid boundary near the center of this depression will be higher than in the undisturbed parts as a result of the finite thermal conductivity of the crystal. Since at constant overall volume the helium will melt in higher temperature regions and crystallize in the other parts, the stochastic deformation will grow in amplitude instead of decay. As in the case of the electrohydrodynamic instability those deformations with a wave vector close to the capillary length will grow preferentially. Although this ought to be a rather general phenomenon when heat flows across a solid-melt interface, the high sensitivity of helium crystals to even minute differences in the chemical potential may favor such an effect. Certainly more investigations are necessary to establish this interpretation of the surface structures in Fig. 13.

IV. Summary

The growth coefficient of rough ^4He crystal surfaces strongly depends on temperature: The results presented here together with the data of other groups show that it spans over 5 orders of magnitude between 0.5 and 1.6 K. Our measurements concentrate on the higher temperature range, where the mean free path of thermal excitations in the liquid is short and the system is therefore in the hydrodynamic regime. The temperature dependence in this range is found to be the same as in the lower temperature ballistic regime, namely $(m_4 K)^{-1} \propto e^{-\Delta E/k_B T}$, with values of ΔE close to the roton energy both for hcp and bcc crystals. The growth of ^4He crystals in the investigated temperature range therefore appears to be governed by the number of rotons in the liquid. This result for the hydrodynamic regime is at variance with theories for the growth coefficient based on the model of roton reflection from the interface, but the discrepancy is removed when ordering in the structure of the liquid close to the interface is taken into account [14]. As a further result, measurements

of the hcp phase have shown that the absolute value of the growth coefficient depends on crystal orientation, with an anisotropy of about a factor of 2.5 between the $(10\bar{1}0)$ and the (0001) surface. As before, this could be interpreted as being due to the local order close to the interface, but a quantitative theory is still missing.

We appreciate valuable discussions with S. Balibar, B. Castaing, D.O. Edwards and A.Ya. Parshin. This work was supported by the Deutsche Forschungsgemeinschaft.

References

1. See, e.g., Jackson, K.A.: In: Crystal growth and characterization. Uedo, R., Mullin, J.B. (eds.), pp. 21–32. Amsterdam: North Holland 1975
2. Müller-Krumbhaar, H.: In: Festkörperprobleme XIX. pp. 1–20. Braunschweig: Vieweg 1979; In: Lectures at the Nato Summer School, Cargèse, 1982
3. Balibar, S., Castaing, B.: J. Phys. (Paris) Lett. **41**, 329 (1980); Wolf, P.E., Gallet, F., Balibar, S., Rolley, E., Nozieres, P.: J. Phys. (Paris) **46**, 1987 (1985)
4. Avron, J.E., Balfour, L.S., Kuper, C.G., Landau, J., Lipson, S.G., Schulman, L.S.: Phys. Rev. Lett. **45**, 814 (1980)
5. Keshishev, K.O., Parshin, A.Ya., Babkin, A.V.: Sov. Phys. JETP **30**, 56 (1979); Sov. Phys. JETP **53**, 362 (1981)
6. Castaing, B., Balibar, S., Laroche, C., Nozieres, P.: J. Phys. **41**, 897 (1980)
7. Huber, T.E., Maris, H.J.: Phys. Rev. Lett. **47**, 1907 (1981); J. Low Temp. Phys. **48**, 463 (1982); J. Low Temp. Phys. **48**, 99 (1982)
8. Savignac, D., Leiderer, P.: Phys. Rev. Lett. **69**, 1869 (1982)
9. Wanner, M., Leiderer, P.: Phys. Rev. Lett. **42**, 315 (1979)
10. Bodensohn, J., Leiderer, P., Savignac, D.: In: Proceedings of the 4th International Conference on Phonon Scattering in Condensed Matter (1983)
11. Leiderer, P.: Physica **126B**, 92 (1985)
12. Balibar, S., Castaing, B., Laroche, C.: J. Phys. Lett. **41**, L-283 (1980)
13. Wiechert, H., Lauter, H.J., Stühn, B.: J. Low Temp. Phys. **48**, 3/4 (1982)
14. Castaing, B.: J. Phys. (Paris) Lett. **45**, 233 (1984)
15. Andreev, A.F., Knizhnik, V.G.: Sov. Phys. JETP **56**, 226 (1982)
16. Bowley, R.M., Edwards, D.O.: J. Phys. (Paris) **44**, 723 (1983)
17. Broughton, J.A., Bonissent, A., Abraham, F.F.: J. Chem. Phys. **74**, 4029 (1981)
18. Wolf, P.E., Balibar, S., Gallet, F.: Phys. Rev. Lett. **51**, 1366 (1983)
19. Dietrich, O.W., Graf, E.H., Huang, C.H., Passell, L.: Phys. Rev. **A5**, 1377 (1972)

J. Bodensohn
K. Nicolai
P. Leiderer
Fachbereich Physik
Johannes-Gutenberg-Universität
Staudinger Weg 7
D-6500 Mainz
Federal Republic of Germany